Predictive early gene signature during mouse Bhas 42 cell transformation induced by synthetic amorphous silica nanoparticles

Anaïs Kirsch, Hélène Dubois-Pot-Schneider, Caroline Fontana, Hervé Schohn, Laurent Gaté, Yves Guichard

Predictive early gene signature during mouse Bhas 42 cell transformation induced by synthetic amorphous silica nanoparticles

Anaïs Kirsch[1,2], Hélène Dubois-Pot-Schneider[2], Caroline Fontana[1], Hervé Schohn[2], Laurent Gaté[1] & Yves Guichard[1*]

[1]Institut National de Recherche et de Sécurité (INRS), 1, rue du Morvan - CS 60027 – 54519 Vandoeuvre Cedex

[2]Université de Lorraine, CNRS, CRAN, F-54000 Nancy, France

Anaïs Kirsch: anais.kirsch@inrs.fr

Hélène Dubois-Pot-Schneider: helene.dubois-pot-schneider@univ-lorraine.fr

Caroline Fontana: caroline.fontana@inrs.fr

Hervé Schohn: herve.schohn@univ-lorraine.fr

Laurent Gaté: laurent.gate@inrs.fr

Yves Guichard: yves.guichard@inrs.fr

*Corresponding Author: yves.guichard@inrs.fr

[1]

Abbreviations

SAS: Synthetic amorphous silica nanoparticles; TPA: 12-O-tetradecanoylphorbol-13-acetate; DE: Diatomeous earth; CTA: Cell transformation assays; OECD: Organization for economic cooperation and development; FBS: Fetal bovine serum; EDTA: Ethylenediaminetetraacetic acid; D21: Day 21; DMSO: Dimethyl sulfoxide; RINs: RNA integrity number; FC: Fold change; GSEA: Gene set enrichment analysis; ES: Enrichment score; MSigDB: Molecular signatures database; ACTB: β-Actin; TUBA: α-Tubulin; GAPDH: Glycerldehyde-3-phosphate dehydrogenase; PBS: Phosphate buffer salin; RIPA: Radioimmunoprecipitation assay buffer; SDS PAGE: Sodium dodecyl sulphate poly-acrylamide gel electrophoresis; PVDF: Polyvinylidene difluoride; BSA: Bovin serum albumin; HRP: Horseradish peroxidase; AUNIP: Aurora kinase A and Ninein interacting protein; LGALS7: Galectin-7: LUM: Lumican; IL1RL1: Interleukin1 receptor-like 1; MCM10: Mini Chromosome Maintenance deficient 10; PRL2C: Proliferin; TIMP4: Metallopeptidase inhibitor 4; LOAEL: Lowest observed adverse effect level; IPA: Igenuity pathway analysis; ELISA: Enzyme-linked immunosorbent assay

Highlights

- Synthetic amorphous silica nanomaterials induce transformation of Bhas 42 cells
- Early modulated signaling pathways are linked to cell adhesion and proliferation
- Twelve genes were selected based on their potential role in cell transformation
- These genes may serve as early markers of Bhas 42 cell transformation induced by SAS

Abstract

Synthetic amorphous silica nanoparticles (SAS) are used widely in industrial applications. These nanoparticles are not classified for their carcinogenicity in humans. However, some data still demonstrate a potential carcinogenic risk of these compounds in humans. The Bhas 42 cell line was developed to screen chemicals, as tumor-initiators or -promoters according to their ability to trigger cell-to-cell transformation, in a cell transformation assay. In the present study, we performed unsupervised transcriptomic analysis after exposure of Bhas 42 cells to NM-203 SAS as well as to positive (Min-U-Sil 5® crystalline silica microparticles, and 12-*O*-tetradecanoylphorbol-13-acetate) and negative (diatomaceous earth) control compounds. We identified a common gene signature for 21 genes involved in the early stage of the SAS- Min-U-Sil 5®- or TPA-induced cell transformation. These genes were related to cell proliferation (over expression) and cell adhesion (under expression). Among them, 12 were selected on the basis of their potential impact on cell transformation. RT-qPCR and western blotting were used to confirm the transcriptomic data. Moreover, similar gene alterations were found when Bhas 42 cells were treated with two other transforming SAS. In conclusion, the results obtained in the current study highlight a 12-gene signature that could be considered as a potential early "bio-marker" of cell transformation induced by SAS and perhaps other chemicals.

Keywords: silica particles, nanomaterials, Bhas 42 cells, cell transformation, transcriptomic profile

1. Introduction

Synthetic amorphous silica (SAS) is one of the nanomaterials produced and used most widely in industrial applications, with worldwide production estimated at 1.5 million tons. SAS are mainly produced in industry by either a wet process, to yield precipitated SAS, or a thermal process, to form pyrogenic SAS [1]. Being a nanostructured material, SAS possesses appealing properties such as a large specific surface area, and it has been used for decades in various industrial applications such as chemistry, cosmetics, pharmaceuticals and food [2].

Several studies have reported toxicological effects of SAS, including oxidative stress, cytotoxicity, inflammation and genotoxicity [1, 3]. Precipitated and pyrogenic SAS have also been found to cause increased dose-dependent changes in lung inflammation after repeated intratracheal instillations in rats [4]. However, little is known about the carcinogenic potential of SAS. Unlike crystalline silicas, which are classified as carcinogenic in humans by the International Agency for Research of Cancer, SAS are not classified as carcinogenic due to a lack of data [5]. Two long-term carcinogenesis studies with SAS have been published to date, showing that repeated intratracheal instillations of pyrogenic SAS in rats increased the incidence of lung tumors [6, 7]. Recently, we showed that precipitated and pyrogenic SAS (NM-200, NM-201 NM-202 and NM-203) induced the transformation of Bhas 42 cells in cell transformation assays (CTA) [8].

The Bhas 42 CTA is one of the existing *in vitro* models for cell transformation [9]. Cell transformation is an early event of *in vivo* multistep carcinogenesis, involving changes in the morphological properties of normal to neoplastic cells. Cell transformation assays simulate *in vivo* initiation and promotion stages of carcinogenesis and can be used to distinguish tumor initiators from tumor promoters [9-11].

The transgenic Bhas 42 cell line, established from Balb/c 3T3 cells [12], contains several copies of the v-Ha-*ras* gene. Similar to the parental Balb/c 3T3 cells, untransformed Bhas 42 cells grow to confluence, forming a cell-density-dependent monolayer. However, after exposure to a transforming chemical, cells become morphologically altered and form discrete foci on the confluent monolayer. Bhas 42 cells can respond to a tumor-promoter without undergoing preliminary treatment with an initiator, in contrast with the two-stage Balb/c 3T3 CTA [13, 14]. The Bhas 42 CTA was validated with a number of known carcinogens and non-carcinogens [15] and is now the subject of a guidance document produced by the Organization for Economic Cooperation and Development [16].

Cell transformation depends on a cascade of complex events that occur within a few hours or weeks [17]. To decipher these processes, the transcriptomic approach allows access to a global gene signature of cellular function after cell exposure to chemicals [18]. The aim of this study was thus to use transcriptomic analysis to identify an early gene signature for Bhas 42 cell transformation that is shared by an SAS, a crystalline silica and the tumor promoter 12-*O*-tetradecanoylphorbol-13-acetate (TPA). Based on previous data [8], the transcriptomic procedure was carried out after Bhas 42 cell exposure to the SAS NM-203, which in the previous study induced the highest level of cell transformation. In addition, the crystalline silica Min-U-Sil 5® and the amorphous silica DE (diatomaceous earth) were used as transforming and non-transforming reference particles, respectively [19].

2. Materials and methods

2.1 Cell culture

Bhas 42 cells were obtained from Harlan Laboratories (Rossdorf, Germany). Cells were grown in Eagle's minimum essential medium (Gibco™, Thermo Fisher Scientific, Villebon sur Yvette, France), supplemented with 1 % (v/v) antibiotic (Streptomycin and Penicillin, Gibco™) and 10 % (v/v) fetal bovine serum (FBS, Dutscher, Brumath, France) (M10F) in a humidified 5 % CO_2 incubator at 37 °C up to about 70 % confluence. Cells were recovered using a 0.25 % (v/v) Trypsin/EDTA solution (Invitrogen) and sub cultured in Dulbecco's modified Eagle's medium/Ham's F12 (Gibco™) supplemented with 1 % (v/v) antibiotic and 5 % (v/v) FBS (DF5F) at about 70 % of the confluence to be used in the CTA.

2.2 Cell transformation and cell survival assays

The CTA in promotion condition, originally proposed by the OECD [16], was modified as described previously [8] (Supplementary Fig. A.1). Cells were seeded at 1460 cells/cm² in a six-well plate on day 0 and the cells were treated once on day 4 (D4). The cells were then post-cultivated in fresh medium until day 21 (D21), receiving a medium change on days 7 (D7), 10 and 14. Cells were fixed with ethanol (Fisher, France) and stained with a 5 % (v/v) Giemsa solution (Thermo Fisher Scientific) on D21. The transformed foci were evaluated according to the morphological criteria recommended by

the OECD (2016). For each experiment, the mean number of transformed foci per treatment group was determined from six replicate wells.

Cell cytotoxicity was assessed by cell survival assay on D7 performed as follows: cells were suspended by trypsination and stained with a mixture of acridine orange/propidium iodide (Sigma-Aldrich, Saint Quentin Fallavier, France), and then counted using a Cellometer® (Vision Nexcelom Bioscience, Lawrence, MA). Cell survival was expressed as the percentage of living cells after cell exposure to the chemical per living cells counted in the untreated condition.

2.3 Particles and cells treatments

Silica nanoparticles (NM-200, NM-201, NM-202, and NM-203) were obtained from the Joint Research Centre nanomaterials repository (Ispra, Italy) (Supplementary Table A.1). Min-U-Sil 5® was obtained from US Silica Co and DE was obtained from the European Coal and Steel Community (Paris, France). Thorough physical and chemical characterizations of SAS, Min-U-Sil 5® and DE batches have been described previously [8]. For cell treatment, vials containing particles suspended in sterile deionized water (19.2 mg/mL) were sonicated for 5 min at 10 % amplitude in the cup horn of a 400 W Branson Sonifier S-450D (Branson Ultrasonics Corp, Danbury, CT). Serial dilutions were prepared in water from the sonicated suspension. Each dilution was added to DF5F to give a final concentration of water of 2 % (v/v). Final particle concentrations were expressed as mass per cell culture surface area and ranged from 1 µg/cm^2 to 40 µg/cm^2 depending on the assay. TPA (Sigma-Aldrich) was diluted at 0.05 µg/mL in dimethyl sulfoxide (DMSO, Sigma Aldrich) at a final concentration of 0.1 % (v/v).

2.4 RNA extraction and quality control

For both transcriptomic analysis and RT-qPCR, RNA samples were obtained from four independent experiments. In both cases, total RNA was extracted from treated cells on D6 using the RNeasy Plus Mini Kit (Qiagen, Courtaboeuf, France) according to the manufacturer's instructions. RNA purity and integrity were evaluated with an Agilent Bioanalyser (Agilent Technologies). All RINs (RNA integrity numbers) were greater than 8.

2.5 Transcriptomic analysis

Transcriptomic analysis was carried out with total RNA extracted from cells exposed from D4 to D6 to NM-203 (1, 2 and 5 µg/cm²), Min-U-Sil 5® (20 µg/cm²), DE (5 µg/cm²), TPA (0.05 µg/mL) and their associated vehicle control: 2% (v/v) H_2O for NM-203, Min-U-Sil 5® and DE and 0.1% (v/v) DMSO for TPA. One hundred nanograms of total RNA were used to synthesize double-stranded cDNA and cyanine labeled cRNA using the one-color low-input QuickAmp labeling kit (Agilent Technologies) according to the manufacturer's instructions. cRNA were purified using the RNeasy Plus Mini Kit (Qiagen). cRNA were hybridized to an Agilent Sureprint G3 mouse gene expression v2 8x60k pangenomic microarray. Gene expression data were extracted using Feature Extraction 11.0.1.1 and analysed using GeneSpring 14.9-GX-PA software (Agilent Technologies).

The microarray data obtained in this study were deposited in the NCBI Gene Expression Omnibus and were accessible through GEO (https://www.ncbi.nlm.nih.gov/geo/query/acc.cgi?acc=GSE133279).

To determine the dose effect of NM-203 (at 1, 2 and 5 µg/cm²), a one-way ANOVA, followed by a Tukey post-hoc test and a Benjamini-Hochberg multiple correction test, was performed with a p-value < 0.005 and a Fold Change (FC) > 4. To determine genes deregulated significantly between two conditions (treatment *vs* control (H_2O or DMSO)), an unpaired t-test (Benjamini-Hochberg correction) with a p-value < 0.05, FC > 2 or with a p-value < 0.005, FC > 4 was used.

2.6 Bioinformatic analysis

Microarray data were clustered with Gene Cluster 3.0 software and the tree was visualized using TreeView 1.6 software. An uncentred correlation was applied for the measure of similarity and gene clustering was based on complete linkage. Biological functions corresponding to the main clusters were evaluated using the FuncAssociate 2.0 web-based tool.

For treatment signature analyses, top canonical pathways were identified with ingenuity pathway analysis (IPA) software (Ingenuity Systems, Redwood City, CA, USA) and signature enrichment analysis was conducted with Gene Set Enrichment Analysis (GSEA) software by using the Java-tool developed at the Broad Institute (Cambridge, MA, USA) on a normalized and filtered list of genes. Unsupervised GSEA was performed on the whole C2 collection of curated gene sets from the

molecular signatures database (MSigDB). Enrichment score (ES) was determined after 1000 permutations.

2.7 Gene expression analysis by RT-qPCR

Total RNA was reverse-transcribed with the iScript™ cDNA synthesis Kit (BioRad, Marnes-la-Coquette, France) following the manufacturer's protocol. Real-time PCR was performed with CFX96 Touch™ (BioRad) in the presence of iQ™ SYBR® Green Supermix (BioRad) and PrimePCR Assay (or 2.5 µM of each primer (Eurogentec, Anger, France) (Supplementary Table A.2).

Amplification was performed following the manufacturer's protocol: the annealing temperature was 60 °C for all pairs of primers. PCR results were analyzed using the SQ method. The results were expressed as relative to those of control cells treated with H_2O or DMSO, arbitrarily set to 1. *ACTB* (beta-Actin), *TUBA* (alpha-Tubulin), and *GAPDH* (glyceraldehyde-3-phosphate dehydrogenase) were used as housekeeping genes whose values have been averaged (geometric mean).

2.8 Protein analysis

Bhas42 cells were treated as stated before. On D6, cell medium supernatants were harvested and stored at -80 °C. Cell layers were washed 3 times with cold PBS (1.44 mM Na_2HPO_4, 0,2 mM KH_2PO_4 containing 0.148 M NaCl, 2 mM KCl) and scraped with a rubber policeman with ice-cold RIPA buffer (50 mM Tris-HCl,pH 8, containing 150 mM NaCl, 1 % (v/v) Triton X-100, 0.5 % (w/v) sodium deoxycholate, 0.1 % (w/v) SDS and 1 % (v/v) protease and phosphatase inhibitor mixture (Thermo Scientific). The homogenates obtained were placed under agitation for 30 min at 4 °C, then centrifuged at 16000 g for 20 min at 4 °C. Supernatants were collected and stored at -80 °C. Protein concentration was measured in each sample and corresponding cell medium supernatant, using bovine serum albumin as a standard (Protein quantification kit, Sigma-Aldrich).

Proteins (50 µg) of whole cell homogenates or 20 µl of corresponding cell medium supernatants were resolved in 4–20 % SDS PAGE (CriterionTM Tris-Glycine eXtended Stain-Free Protein Gel, BioRad) and transferred onto polyvinylidene difluoride (PVDF) membranes (BioRad), using semi-dry transfert (BioRad). The saturation step was performed in PBS-T buffer (PBS supplemented with 0.1 % (v/v) Tween 20) containing 5 % (w/v) non-fat milk for 1 h at room temperature. Antibody solutions were prepared in PBS-T containing 5 % (w/v) BSA) and membranes were incubated overnight at 4 °C with

gentle agitation. Primary antibodies were directed against Aurora kinase A and Ninein interacting protein (AUNIP, Cell Signaling Technology, Ozyme, Saint-Cyr-l'École, France; 1: 500), Galectin-7 (ab206435; Abcam, Paris, France; 1: 1000), Lumican (LUM, 7076P2, Cell Signaling Technology; 1: 250), Interleukin1 receptor-like 1 (IL1RL1, Cell Signaling Technology, 1: 1000), Mini Chromosome Maintenance deficient 10 (MCM10, Cell Signaling Technology, 1:500), Proliferin (AF1623; R&D System; 1: 1000), Metallopeptidase inhibitor 4 (TIMP4, Abcam; 1: 5000), and β-Actin (4970; Cell Signaling Technology; 1: 10000). Membranes were washed 3 times with PBST, then incubated for 1h at room temperature with either HRP-conjugated anti-goat IgG (1: 5000) or HRP-conjugated anti-rabbit IgG (1: 2000) in PBST containing 5 % (w/v) non-fat milk. Finally, membranes were washed3 times with PBST before chemiluminescence detection (Clarity ™ Western ECL Substrate, BioRad) using ChemiDocTM (ChemiDoc ™ System, BioRad).

Secreted periostin concentration was estimated using a Mouse Periostin/OSF-2 Duoset ELISA kit (R&D Systems, Lille, France). Sample concentration was expressed as ng of periostin/mg of protein.

2.9 Statistics

Statistical analyses were performed using Graph Pad Prism software (Version 8.0.1; Graphpad, San Diego, CA). For CTA and cell survival assays logarithmic transformation was applied to the data. For multiple comparisons, the significance was evaluated by a one-way ANOVA followed by a Dunnett's multiple comparisons test.

An unpaired t-test was used for two by two comparison (treatments *vs*. control (H_2O or DMSO)).

Data are given as a mean ± standard deviation (mean ± SD).

3. Results

3.1 Cytotoxic and transforming effects of NM-203, Min-U-Sil 5®, DE and TPA.

CTAs in promotion condition were performed according to the OECD guidance document [16], except that instead of receiving three treatments during the assay, cells were treated once on Day 4. Cytotoxicity assays were performed on D7 applying the dose range of particles used in the previous study [8]. The cytotoxic effect of NM-203, Min-U-Sil 5® and DE was moderate; the decrease in cell survival was less than 30 % (Supplementary data Table A.3). NM-203 and Min-U-Sil 5® induced a significant dose-response effect on cell transformation (Fig. 1A). The lowest observed adverse effect level (LOAEL) was observed at 5 µg/cm² and 20 µg/cm² for NM-203 and Min-U-Sil 5®, respectively.

TPA at 0.05 µg/ml, used as a positive control, induced cell transformation. In contrast, DE did not show any transforming activity.

3.2 NM-203, Min-U-Sil 5® and TPA induce alteration of genes involved in cell proliferation and cell adhesion

After normalization and filtering of the raw transcriptomic data using the Genespring software, 19,569 probes were listed. Non supervised hierarchical clustering (Fig. 2A) of these 19,569 remaining probes, showed two main branches, dividing the samples into two groups with regards to the transforming potential: a first group with control conditions (ctrl = 2 % (v/v) H_2O or 0.1 % (v/v) DMSO) and non-transforming conditions (DE at 5 µg/cm² and NM-203 at 1 µg/cm²) and a second group including NM-203 at 2 µg/cm² and transforming conditions (NM-203 at 5 µg/cm², Min-U-Sil® (5 µg/cm²), TPA (0.05 µg/ml)). The Min-U-Sil 5® (20 µg/cm²) group was closer to the NM-203 (5 µg/cm²) group than to the TPA (0.05 µg/ml) group. The NM-203 (2 µg/cm²) group, which was a transforming condition in the Bhas 42 CTA performed with three treatments but not with a single treatment [8], seems to induce gene expression modulation even with a single treatment. To study the dose-effect of NM-203, an ANOVA test was performed with a *p*-value lower than 0.005 selected. Genes that were expressed differently in at least one condition (*vs.* control) with a fold change (FC) greater than 4 were selected (supplementary Table A.4). Hierarchical clustering of the 290 differentially expressed genes showed that increasing the concentration of NM-203 led to a higher increase or decrease response at the mRNA level (Fig. 2B). Treeview analysis highlighted co-regulated groups of genes. Interestingly, the upper part of the dendrogram grouped clusters of genes down-regulated after NM-203 treatment (124 genes) and involved in matrix remodeling and cell adhesion, and the lower part of the dendrogram highlighted genes up-regulated after NM-203 treatment (166 genes) and involved in cell proliferation.

Gene set enrichment analysis (GSEA) identified significant enrichments ($p < 0.01$) of signatures for each treatment (Supplementary Table A.5). Comparison of the top 50 signatures highlighted for each treatment showed that 24 % of signatures were common to the three conditions (Fig. 3A). These twelve common signatures are related mainly to proliferation and cancer features (Fig. 3B-C) [20, 21].

To identify genes significantly deregulated by each treatment, an unpaired t-test (Bonferroni FWER correction) with a p-value < 0.05, FC > 2 was used. RNA levels of 1,580 genes were modified after cell treatment by NM203 (5 µg/cm²) (Supplementary Table A.6), 1,044 genes with Min-U-Sil 5®

(Supplementary Table A.7), and 383 genes by TPA (Supplementary Table A.8). Interestingly, NM-203 at 2 µg/cm^2 induced significant changes in the expression of 512 genes (Supplementary Table A.9). IPA analysis on a smaller set of genes (selected with an unpaired t-test with a p-value < 0.005, FC > 4; Supplementary Table A.10-A.13) showed that the former three treatments regulated a number of common pathways involved mainly in cell proliferation (Supplementary Table A.14).

3.3 Comparison of early molecular signature and selection of common genes

Genes significantly highly regulated by NM-203 (5 µg/cm^2), Min-U-Sil 5® and TPA were compared ($p < 0.005$ and FC > 4) (Fig. 4A). Of the 309 genes altered by treatments, a large majority (83 %) were affected by NM-203. Among these, 142 (46 %) were affected solely by NM-203 treatment and 23 (7 %) and 29 genes (9 %) were deregulated by Min-U-Sil 5® and TPA, respectively. Interestingly, 21 common genes were regulated significantly by NM-203 (5 µg/cm^2), Min-U-Sil 5® and TPA ($p < 0.005$, FC > 4). Twelve genes, *CACNA1G, CMBL, ENPP2, GDPD2, HMGCS2, LGALS7, LUM, POSTN, SEMA3G, SPARCL1, TIMP4,* and A230065H16Rik, were underexpressed whereas 9 genes, *RAD51AP1, NLRP2, SGOL1, IL1RL1, PRL2C3, PRL2C5, PRL2C1, AUNIP* and *MCM10* were overexpressed (Fig. 4B). We selected 6 genes known to be involved in cell proliferation (*AUNIP, IL1RL1, MCM10, PRL2C1, PRL2C3 and PRL2C5*) and 6 genes involved in cell-cell adhesion (*LGALS7*, *LUM, POSTN, SEMA3G, SPARCL1,* and *TIMP4*) (Table 1). For all these genes, RT-qPCR results were broadly in line with transcriptomic results and confirmed the dose-effect produced by NM-203 (Table 2).

3.4 Transforming silica nanoparticles NM-200 and NM-202 induce similar changes at the RNA level of the selected genes.

We then assessed whether Bhas 42 cell exposure to other SAS, namely NM-200, NM 201 and NM202, led to cell transformation and involved any changes at the RNA level of the selected genes. NM-200 were slightly cytotoxic at the highest concentration (40 µg/cm^2) while NM-202 decreased cell survival by approximately 50 % at 40 µg/cm^2. NM-201 treatment had no cytotoxic or transforming effect (Fig.1B and supplementary Table A3). Bhas 42 cell exposure to NM-200 (20 µg/cm^2) or NM-202 (20 µg/cm^2) led to similar expression patterns as those obtained when cells were treated with NM203 (5 µg/cm^2), *i.e.* an increase in RNA levels of *AUNIP, IL1RL1*, *MCM10, PRL2C1*, *PRL2C3* and

PRL2C5, and a decrease for *LGALS7, LUM*, *POSTN*, *SEMA3G*, *SPARCL1*, and *TIMP4*. In contrast, cells exposed to NM-201 showed no change in each gene expression (Fig. 5).

3.5 Changes at the protein level

We assessed whether the increase at the mRNA level of selected genes was related to corresponding changes at the protein level. We performed Western blotting procedure or ELISA with available commercial antibodies (Fig. 6). Among the antibodies tested, we could not estimate the respective protein expression levels of AUNIP, LUM, TIMP4, due to a lack of a specific antibody (presence of a non-specific band) or due to low immune signals.

Among the list of genes with increased expression after Bhas42 cell treatment, IL1RL1, as the receptor of IL33, was detected with an estimated band at 37 kDa, in all conditions tested, with slight changes between control and treated cell homogenates. Moreover, glycosylated IL1R1 could be secreted as a response to reduce receptor signaling by IL33 [22]. Glycosylated IL1R1 appears as a broad band around 50 kDa, but slight changes in the secreted receptor levels were observed. Proliferin, as a growth hormone /prolactin related secreted glycoprotein [23, 24], encoded by *PRL2C1*, *PRL2C3*, *PRL2C5* genes, was detected in whole cell homogenate and in cell medium supernatant as a single band at 60 KDa. As shown in Figure 6, the protein was secreted in all conditions tested, but we failed to detect it in homogenates prepared from cells treated with H_2O, DMSO, NM-201, low concentrations of NM-203 (1 and 2 µg/cm^2), and DE, supporting the concept that proliferin is continuously secreted. In contrast, the protein was detected in cell homogenates prepared from cells exposed to NM-200, NM-202, NM-203 (2 and 5 µg/cm^2), Min-U-Sil 5®, and TPA, suggesting that the synthesis rate of the protein is enhanced under these experimental conditions.

Among the genes showing decreased expression after cell exposure to SAS, periostin, involved in cell matrix adhesion and epithelial mesenchymal transition [25], was measured by ELISA in cell medium supernatants. Protein levels were lowered when Bhas 42 cells were treated with 20 µg/cm^2 of NM-200, NM-202 and Min-U-Sil 5®, 5 µg/cm^2 NM-203 and 0.05 µg/ml TPA, in agreement with the observed decrease in mRNA levels. However, protein levels were also low when cells were exposed to NM-201 (20 µg/cm^2) or NM-203 (2 µg/cm^2), whereas no change was found when cells were treated with 1 µg/cm^2 NM-203 or 5 µg/cm^2 DE (Fig. 6). MCM10, involved in DNA recombination and elongation [26] was also detected in whole cell homogenate as a band estimated at 100 kDa. We did not observe any

significant changes at the protein level whatever the treatment tested. These results could be related to the experimental design of the CTA, since, from the beginning of cell treatment on D4, Bhas 42 cells continue to undergo cell division until D6, maintaining a high level of MCM10, a protein necessary for DNA synthesis [26]. Finally, galectin 7, involved in cell-cell or cell-matrix interaction [27], was detected in whole cell homogenates with a band estimated at 37 kDa (Fig. 6). Galectin 7 levels were lowered when cells were treated with NM-200, NM-202, NM-203 (2 and 5 µg/cm^2), and Min-U-Sil 5® (20 µg/cm^2), whereas no change was found in the other conditions tested.

4. Discussion

4.1 Selection of genes as possible markers of SAS-induced Bhas42 cell transformation

Although SAS are extensively produced and used, few studies have focused on their transforming or carcinogenic potential [1, 3]. In a previous study, the transforming properties of the NM-200, NM-201, NM-202 and NM-203 SAS were revealed in the Bhas 42 CTA using the promotion assay. In order to decipher the molecular changes during the Bhas 42 CTA, an unsupervised transcriptomic analysis was performed following exposure of cells to SAS and control chemicals for 48h. In this treatment time, NM-203 and Min-U-Sil 5® have been shown to induce epigenetic effects in Bhas 42 cells in the promotion assay [28]. We therefore hypothesized that this treatment time could highlight earlier gene changes involved in Bhas 42 cell transformation. The lowest concentrations of chemicals able to induce cell transformation without inducing cytotoxicity were selected in transcriptomic and RT-qPCR assays. The expression of 21 genes was altered by the three treatments, NM-203, Min-U-Sil 5® and TPA. Among them, twelve genes, whose involvement in cell proliferation and adhesion has been proven (Table 1), were selected as putative markers of the transforming properties of SAS nanomaterials. To confirm this hypothesis, we tested the NM-200, NM201 and NM-202 SAS (Fig. 1B and 5). Similar changes in the RNA levels of each selected gene were obtained with NM-200 and NM-202, supporting the hypothesis that the genes in this set are potential markers of SAS-induced cell transformation. However, NM-201 treatment induced no change in the expression of these 12 genes (Fig. 5). This could be explained by the fact that, unlike the three repeated treatments of NM-201 [8]), a single treatment did not cause Bhas 42 cell transformation. One reason for this could be that NM-

201 has a lower BET-SSA than the other SAS (140 *vs* ≈ 200 g/cm^2) (Table A.1). Indeed, the toxicity of nanomaterials is often associated with their high specific surface area, which results in a high reactivity with the biological environment. In addition, we demonstrated concomitant changes in the mRNA and protein levels of several genes, such as galectin 7, periostin or proliferin. However, a concordance between mRNA and protein levels was not systematically found. It is possible that regulation mechanisms of protein synthesis and processing may occur.

Interestingly, the increase in *PRL2Ci* mRNA levels, encoding proliferin, was observed in CTA performed with BALB c/3T3 cells [13, 14] and C3H/10T1/2 cells [29, 30] treated with various chemicals including amorphous silica particles (silica gel of 5 µm). Proliferin expression was considered as a predictive biomarker of cell transformation [13, 14]. However, even though the expression of three members of the proliferin gene family, *PRCl2C2,3,5,* was upregulated, proliferin was revealed as a single band by western blotting. On the other hand, c-myc upregulation was also linked to C3H/10T1/2 [29] and Bhas 42 cell transformation [28]. In the latter, *C-MYC* mRNA and protein levels increased after cell treatment with NM-203 and Min-U-Sil 5® over 2 days. Similar changes in mRNA level were also found in the present study with $p < 0.005$ and $FC > 4$ (Supplementary Tables A10-A11). Accordingly, Bhas 42 cell transformation is associated with early increased *C-MYC* expression, but not in the late phase of SAS-induced cell transformation as shown previously [28]. These results, among others [14, 31], confirm that markers of transformation must be identified in the early steps of the processes. Finally, epigenetic modifications have also been related to cell transformation as recently reviewed [32]: it has been shown that cadmium chloride, methyl carbamate and lithocholic acid (three transforming compounds) can induce genome-wide DNA methylation changes in Bhas 42 cells [33]. Moreover, Seidel *et al*. proposed that the transforming activity of the crystalline silica Min-U-Sil 5® in Bhas 42 cells was related to early epigenetic DNA methylation [28].

4.2 Gene expression changes after SAS exposure

The transcriptomic analyses showed that NM-203, Min-U-Sil 5® and TPA are related to increases in the expression of genes involved in cell cycle progression, to DNA recombination, to decreased matrix and remodeling functions, and to cell-cell adhesion. This is in accordance with different transcriptomic studies that have used the BALB c/3T3 cell line in the context of CTA [14, 31]. Moreover, *IL1RL1, LGALS7*, *LUM, MCM10, POSTN and SPARCL1* have all been associated with SAS toxicity. For

example, *IL1RL1* has been found to be involved in inflammasome activation induced by crystalline silica in human lung epithelial cells (BEAS2B) and in primary human bronchial epithelial cells (NHBE) [34, 35]. An increase in the expression of *LUM, MCM10, POSTN, SPARCL1* and *IL1RL1* has been observed in RAW 264, 7 cells (murine macrophages cells) treated with SAS (10 or 300 nm) [34]. Pisani et al. showed overexpression of *LUM, LGALS7* and *MCM10* in FE1 cells treated with AEROSIL 200® (NM-203) [36]. In addition, variations in gene expression related to the cell cycle or cell adhesion were found after treatment of the lung epithelial cell line FE1 exposed for 24h to 12, 15 and 20 nm SAS [37]. Furthermore, pathway analysis has revealed that protein contents in the adenocarcinomic human alveolar basal epithelial cell line A549 treated with Min-U-Sil 5® for 24h are associated with cell proliferation [38].

4.3 Gene expression changes related to cancer progression

All of the genes selected are known to be involved in cancer progression. Six of the genes were overexpressed by the three treatments. In previous studies, for example, overexpression of *IL1RL1*, has been observed in tumor cells from human colon cancer [39], the respective expression of the *PRL2C* gene family was increased in fallopian tube epithelium derived ovarian cancer cells [40], *MCM10* was increased in medulloblastoma, urothelial carcinomas, prostate cancer and breast cancer [41-44] and finally, *AUNIP* was overexpressed in various brain tumors [45]. Conversely, respective expression of the 6 selected genes was downregulated by the three treatments in this study. In previous studies, expression of *LUM, POSTN, SPARCL1, LGALS7*, and *TIMP4*, all involved in cell-cell adhesion, was found to be lowered in various cancers: *LGALS7* expression was decreased in cervical cancer, colon cancer, gastric cancer and in malignant melanoma [27, 46-48]; *LUM* was downregulated in various human cancer cell lines [48,49,50], *POSTN* expression was likewise downregulated in bladder and lung cancer [49]; low expression of *SPARCL1* has been shown to be associated with tumor progression in human gastric, breast and prostate cancers [50-52], and expression of *TIMP4* has been found to be low in malignant peripheral nerve sheath tumors associated with neurofibromatosis type 1 [53]. Moreover, some gene expression changes observed in this study are related to cancer progression. For example, *SEMA3G* expression decreased under our experimental conditions. In contrast, overexpression of *SEMA3G* limits the progression of breast cancer or melanoma cells or the migration and invasion of glioma cells [54, 55]. GSEA analysis also revealed an

overall enrichment of gene signatures in response to treatment with NM-203, Min-U-Sil 5® and TPA. Among the signatures found, SAS exposure was related to the response to estradiol and prostaglandin and to G2/M arrest by methoxyestradiol and oligodendrocyte differentiation. Estrogen is an important causal factor in breast cancer [56].

5 Conclusion

Using an unsupervised transcriptomic approach, we have identified 12 genes of Bhas 42 cells that are potentially involved in the transforming effect of SAS. The selected genes were mainly related to positive regulation of cell proliferation and negative regulation of cell adhesion. For the first time, this set of genes can be proposed as an *in vitro* RT-qPCR screening assay for assessment of the early stages of SAS-induced Bhas 42 cell transformation. Our analysis will be extended to other nanomaterials and chemicals in order to strengthen the predictivity of this early gene signature.

Acknowledgements

The authors would like to thank Dr Aurélie Remy for performing the statistical analysis of our results, Hami Musaoglu for his technical help, Dr O. Joubert for the use of his transcriptomics facility, and Prof. S.N. Thornton and Dr. Alice Williams for proof-reading the English in the manuscript.

This work has been funded by the French National Fund for the Prevention of Occupational Accidents and Diseases

428

429 **Table 1:** Characteristics of the selected genes

Gene symbol	Gene title	Gene ontology	Protein localisation	Expression level	References
AUNIP	Aurora Kinase A And Ninein Interacting Protein	Aurk-A interaction during cell cycle	Cytoplasm	Up	[45]
IL1RL1	Interleukin-1 receptor-like 1	Immune response	Plasma membrane	Up	[22]
LGALS7	Galectin-7	Cell-cell and/or cell-matrix interactions	Extracellular space	Down	[57]
LUM	Lumican	Extracellular matrix organization	Extracellular space	Down	[58]
MCM10	Mini-chromosome Maintenance 10	DNA replication	Nucleus	Up	[59]
POSTN	Periostin	Cell adhesion	Extracellular space	Down	[60]
PRL2C1	Prolactin family 2, subfamily c, member 1	Positive regulation of cell proliferation	Extracellular space	Up	[24], [23]
PRL2C3	Prolactin family 2, subfamily c, member 3	Positive regulation of cell proliferation	Extracellular space	Up	[24], [23]
PRL2C5	Prolactin family 2, subfamily c, member 5	Positive regulation of cell proliferation	Extracellular space	Up	[24], [23]
SEMA3G	Semaphorin-3G	Endothelial cell migration	Cytoplasm	Down	[61]
SPARCL1	Secreted protein acidic and rich in cysteine like protein 1	Cell adhesion	Extracellular space	Down	[62]
TIMP4	Metalloproteinase inhibitor 4	Inhibitor of metalloproteinase	Extracellular space	Down	[63]

430
431

Table 2: Fold change value* and correlation between microarray data and RT-qPCR results

Gene symbol		NM-203 (1 µg/cm²)	NM-203 (2 µg/cm²)	NM-203 (5 µg/cm²)	Min-U-Sil 5® (20 µg/cm²)	DE (5 µg/cm²)	TPA (0.05 µg/ml)	*r*
AUNIP	*Microarray*	1.87	5.90	6.22	5.02	1.37	4.74	0.742
	RT-qPCR	1.10	1.70	7.06	2.94	1.38	4.23	
IL1RL1B	*Microarray*	1.64	3.74	4.60	5.06	1.66	4.99	0.844
	RT-qPCR	1.30	1.69	5.88	3.78	1.83	4.76	
LGALS7	*Microarray*	0.81	0.68	0.10	0.16	0.63	0.29	0.961
	RT-qPCR	0.69	0.42	0.02	0.06	0.75	0.09	
LUM	*Microarray*	0.64	0.70	0.11	0.23	0.55	0.28	0.928
	RT-qPCR	0.49	0.33	0.05	0.06	0.67	0.16	
MCM10	*Microarray*	1.64	5.26	7.29	6.27	1.25	4.74	0.846
	RT-qPCR	1.27	2.08	8.50	3.94	1.48	3.82	
POSTN	*Microarray*	0.53	0.35	0.09	0.10	0.47	0.08	0.969
	RT-qPCR	0.66	0.31	0.04	0.04	0.71	0.03	
PRL2C1	*Microarray*	1.49	3.94	18.95	17.46	1.60	13.12	0.962
	RT-qPCR	2.10	4.17	54.40	53.26	3.44	20.00	
PRL2C3	*Microarray*	1.63	5.42	22.82	22.73	1.61	20.26	0.954
	RT-qPCR	1.45	3.10	29.11	29.64	2.30	14.75	
PRL2C5	*Microarray*	1.64	4.81	17.51	17.35	1.61	13.22	0.880
	RT-qPCR	1.97	4.25	18.55	8.44	4.10	15.00	
SEMA3G	*Microarray*	0.60	0.50	0.14	0.27	0.46	0.21	0.889
	RT-qPCR	0.73	0.38	0.13	0.05	0.87	0.09	
SPARCL1	*Microarray*	0.61	0.65	0.04	0.10	0.44	0.27	0.929
	RT-qPCR	0.59	0.32	0.02	0.03	0.64	0.12	
TIMP4	*Microarray*	0.57	0.52	0.11	0.22	0.54	0.12	0.960
	RT-qPCR	0.67	0.45	0.02	0.06	0.79	0.03	

*, fold change values were calculated from results obtained from either microarray or RT-qPCR. Results are expressed with respect to control cells, taken as 1.00. Control cells were treated with H_2O used as the vehicle for respective SAS, DE or Min-U-Sil 5®, and with DMSO as the vehicle for TPA.

Bibliography

[1] D. Napierska, L.C. Thomassen, D. Lison, J.A. Martens, P.H. Hoet, The nanosilica hazard: another variable entity, Particle and Fibre Toxicology, 7 (2010) 39. https://doi.org/10.1186/1743-8977-7-39

[2] ECETOC, ECETOC JACC REPORT, N°51 Synthetic Amorphous Silica (Cas 7631-86-9), (2006) 1-237.

[3] S. Murugadoss, D. Lison, L. Godderis, S. Van Den Brule, J. Mast, F. Brassinne, N. Sebaihi, P.H. Hoet, Toxicology of silica nanoparticles: an update, Archives of Toxicology, 91 (2017) 2967-3010. https://doi.org/10.1007/s00204-017-1993-y

[4] Y. Guichard, M.A. Maire, S. Sebillaud, C. Fontana, C. Langlais, J.C. Micillino, C. Darne, J. Roszak, M. Stepnik, V. Fessard, S. Binet, L. Gate, Genotoxicity of synthetic amorphous silica nanoparticles in rats following short-term exposure. Part 2: intratracheal instillation and intravenous injection, Environmental and Molecular Mutagenesis, 56 (2015) 228-244. https://doi.org/10.1002/em.21928

[5] IARC, Silica, some silicates, coal dust and *para*-Aramid fibrils, IARC Monographs on the Evaluation of Carcinogenic Risks to Humans, 68 (1997) 1-506.

[6] F. Pott, M. Roller, Carcinogenicity study with nineteen granular dusts in rats, European Journal of Oncology, 10 (2005) 249-281. https://doi.org/10.1016/j.etp.2006.06.001

[7] A. Kolling, H. Ernst, S. Rittinghausen, U. Heinrich, Relationship of pulmonary toxicity and carcinogenicity of fine and ultrafine granular dusts in a rat bioassay, Inhalation Toxicology, 23 (2011) 544-554. https://doi.org/10.3109/08958378.2011.594458

[8] C. Fontana, A. Kirsch, C. Seidel, L. Marpeaux, C. Darne, L. Gaté, A. Remy, Y. Guichard, In vitro cell transformation induced by synthetic amorphous silica nanoparticles, Mutation Research/Genetic Toxicology and Environmental Mutagenesis, 823 (2017) 22-27. https://doi.org/10.1016/j.mrgentox.2017.08.002

[9] S. Creton, M.J. Aardema, P.L. Carmichael, J.S. Harvey, F.L. Martin, R.F. Newbold, M.R. O'Donovan, K. Pant, A. Poth, A. Sakai, K. Sasaki, A.D. Scott, L.M. Schechtman, R.R. Shen, N. Tanaka, H. Yasaei, Cell transformation assays for prediction of carcinogenic potential: state of the science and future research needs, Mutagenesis, 27 (2012) 93-101. https://doi.org/10.1093/mutage/ger053

[10] C. Lasne, A. Gentil, I. Chouroulinkov, Two-stage Malignant Transformation of Rat Fibroblasts in Tissue Culture, Nature, 247 (1974) 490-491. https://doi.org/10.1038/247490a0

[11] K. Ohmori, M. Umeda, N. Tanaka, H. Takagi, I. Yoshimura, K. Sasaki, S. Asasda, A. Sakai, H. Araki, M. Asakura, H. Baba, Y. Fushiwaki, S. Hamada, N. Kitou, T. Nakamura, Y. Nakamura, H. Oishi, S. Sasaki, S. Shimada, T. Tsuchiya, Y. Uno, M. Washizuka, S. Yajima, Y. Yamamoto, E. Yamamura, T. Yatsushiro, An inter-laboratory collaborative study by the Non-Genotoxic Carcinogen Study Group in Japan, on a cell transformation assay for tumour promoters using Bhas 42 cells, Alternatives to Lab Animals, 33 (2005) 619-639. https://doi.org/10.3390/cancers10090282

[12] K. Sasaki, H. Mizusawa, M. Ishidate, Isolation and characterization of ras-transfected BALB/3T3 clone showing morphological transformation by 12-O-tetradecanoyl-phorbol-13-acetate, Japanese Journal of Cancer Research, 79 (1988) 921-930. https://doi.org/10.1111/j.1349-7006.1988.tb00056.x

[13] H. Maeshima, K. Ohno, S. Nakano, T. Yamada, Validation of an in vitro screening test for predicting the tumor promoting potential of chemicals based on gene expression, Toxicology in Vitro, 24 (2010) 995-1001. https://doi.org/10.1016/j.tiv.2009.12.013

[14] H. Maeshima, K. Ohno, Y. Tanaka-Azuma, S. Nakano, T. Yamada, Identification of tumor promotion marker genes for predicting tumor promoting potential of chemicals in BALB/c 3T3 cells, Toxicology in Vitro, 23 (2009) 148-157. https://doi.org/10.1016/j.tiv.2008.10.005

[15] A. Sakai, K. Sasaki, D. Muramatsu, S. Arai, N. Endou, S. Kuroda, K. Hayashi, Y.M. Lim, S. Yamazaki, M. Umeda, N. Tanaka, A Bhas 42 cell transformation assay on 98 chemicals: the characteristics and performance for the prediction of chemical carcinogenicity, Mutation Research/Genetic Toxicology and Environmental Mutagenesis, 702 (2010) 100-122. https://doi.org/10.1016/j.mrgentox.2010.07.007

[16] OECD, Guidance Document On the In Vitro Bhas 42 Cell Transformation Assay Series on Testing & Assessment No. 231, ENV/JM/MONO(2016)1, OECD Publishing, Paris, (2016).

[17] L.A. Loeb, C.C. Harris, Advances in chemical carcinogenesis: a historical review and prospective, Cancer Res, 68 (2008) 6863-6872. https://doi.org/10.1158/0008-5472.CAN-08-2852

[18] S.J. Sturla, A.R. Boobis, R.E. FitzGerald, J. Hoeng, R.J. Kavlock, K. Schirmer, M. Whelan, M.F. Wilks, M.C. Peitsch, Systems Toxicology: From Basic Research to Risk Assessment, Chemical Research in Toxicology, 27 (2014) 314-329. https://doi.org/10.1021/tx400410s

[19] Z. Elias, O. Poirot, M.C. Daniere, F. Terzetti, A.M. Marande, S. Dzwigaj, H. Pezerat, I. Fenoglio, B. Fubini, Cytotoxic and transforming effects of silica particles with different surface properties in Syrian hamster embryo (SHE) cells, Toxicology in Vitro, 14 (2000) 409-422. https://doi.org/10.1016/S0887-2333(00)00039-4

[20] D. Lindgren, F. Liedberg, A. Andersson, G. Chebil, S. Gudjonsson, Å. Borg, W. Månsson, T. Fioretos, M. Höglund, Molecular characterization of early-stage bladder carcinomas by expression profiles, FGFR3 mutation status, and loss of 9q, Oncogene, 25 (2006) 2685-2696. https://doi.org/10.1038/sj.onc.1209249

[21] M. Vecchi, P. Nuciforo, S. Romagnoli, S. Confalonieri, C. Pellegrini, G. Serio, M. Quarto, M. Capra, G.C. Roviaro, E. Contessini Avesani, C. Corsi, G. Coggi, P.P. Di Fiore, S. Bosari, Gene expression analysis of early and advanced gastric cancers, Oncogene, 26 (2007) 4284–4294. https://doi.org/10.1038/sj.onc.1210208

[22] A. Lingel, T.M. Weiss, M. Niebuhr, B. Pan, B.A. Appleton, C. Wiesmann, J.F. Bazan, W.J. Fairbrother, Structure of IL-33 and Its Interaction with the ST2 and IL-1RAcP Receptors—Insight into Heterotrimeric IL-1 Signaling Complexes, Structure, 17 (2009) 1398-1410. https://doi.org/10.1016/j.str.2009.08.009

[23] J.-W. Wang, Y.-N. Jiang, C.-Y. Huang, P.-Y. Huang, M.-C. Huang, W.T.-K. Cheng, C.-K.J. Shen, Y.-T. Ju, Proliferin enhances microvilli formation and cell growth of neuroblastoma cells, Neuroscience Research, 56 (2006) 80-90. https://doi.org/10.1016/j.neures.2006.05.011

[24] J.T. Fassett, M. Nilsen-Hamilton, Mrp3, a Mitogen-Regulated Protein/Proliferin Gene Expressed in Wound Healing and in Hair Follicles*, Endocrinology, 142 (2001) 2129-2137. https://doi.org/10.1210/endo.142.5.8132

[25] M.-O. Riener, F.R. Fritzsche, C. Soll, B.C. Pestalozzi, N. Probst-Hensch, P.-A. Clavien, W. Jochum, A. Soltermann, H. Moch, G. Kristiansen, Expression of the extracellular matrix protein periostin in liver tumours and bile duct carcinomas, Histopathology, 56 (2010) 600-606. https://doi.org/10.1111/j.1365-2559.2010.03527.x

[26] E.M. Warren, H. Huang, E. Fanning, W.J. Chazin, B.F. Eichman, Physical Interactions between Mcm10, DNA, and DNA Polymerase α, Journal of Biological Chemistry, 284 (2009) 24662-24672. https://doi.org/10.1074/jbc.M109.020438

[27] J.C. Higareda-Almaraz, J.S. Ruiz-Moreno, J. Klimentova, D. Barbieri, R. Salvador-Gallego, R. Ly, I.A. Valtierra-Gutierrez, C. Dinsart, G.A. Rabinovich, J. Stulik, F. Rösl, B. Rincon-Orozco, Systems-level effects of ectopic galectin-7 reconstitution in cervical cancer and its microenvironment, BMC Cancer, 16 (2016) 680. https://doi.org/10.1186/s12885-016-2700-8

[28] C. Seidel, A. Kirsch, C. Fontana, A. Visvikis, A. Remy, L. Gaté, C. Darne, Y. Guichard, Epigenetic changes in the early stage of silica-induced cell transformation, Nanotoxicology, 11 (2017) 923-935. https://doi.org/10.1080/17435390.2017.1382599
[29] C.L.J. Parfett, T. Marquardt, R. Pilon, Promotion of Morphological Transformation by di-n-butyltin Dichloride in C3H/10T1/2 Cells: Prediction by Prior Expression of Tumour Promoter-Responsive Genes, Food and Chemical Toxicology, 38 (2000) 339-349. https://doi.org/10.1016/S0278-6915(99)00157-X
[30] C.L.J. Parfett, R. Pilon, A.A. Caldeira, Asbestos promotes morphological transformation and elevates expression of a gene family invariably induced by tumor promoters in C3H/10T1/2 cells, Carcinogenesis, 17 (1996) 2719-2726. https://doi.org/10.1093/carcin/17.12.2719
[31] A. Rohrbeck, G. Salinas-Riester, K. Maaser, J. Linge, S. Salovaara, R. Corvi, J. Borlak, Toxicogenomics Applied to In Vitro Carcinogenicity Testing with Balb/c 3T3 Cells Revealed a Gene Signature Predictive of Chemical Carcinogens, Toxicological Sciences, 118 (2010) 31-41. https://doi.org/10.1093/toxsci/kfq246
[32] C.L. Parfett, D. Desaulniers, A Tox21 Approach to Altered Epigenetic Landscapes: Assessing Epigenetic Toxicity Pathways Leading to Altered Gene Expression and Oncogenic Transformation In Vitro, International Journal of Molecular Sciences, 18 (2017) 1179. https://doi.org/10.3390/ijms18061179
[33] S.-H. Hwang, H. Yeom, S.Y. Eom, Y.-M. Lee, M. Lee, Genome-Wide DNA Methylation Changes in Transformed Foci Induced by Nongenotoxic Carcinogens, Environmental and Molecular Mutagenesis, 0 (2019). https://doi.org/10.1002/em.22285
[34] P.M. Peeters, T.N. Perkins, E.F.M. Wouters, B.T. Mossman, N.L. Reynaert, Silica induces NLRP3 inflammasome activation in human lung epithelial cells, Particle and Fibre Toxicology, 10 (2013) 3. https://doi.org/10.1186/1743-8977-10-3
[35] T.N. Perkins, P.M. Peeters, A. Shukla, I. Arijs, J. Dragon, E.F.M. Wouters, N.L. Reynaert, B.T. Mossman, Indications for distinct pathogenic mechanisms of asbestos and silica through gene expression profiling of the response of lung epithelial cells, Human Molecular Genetics, 24 (2015) 1374-1389. https://doi.org/10.1093/hmg/ddu551
[36] C. Pisani, J.-C. Gaillard, V. Nouvel, M. Odorico, J. Armengaud, O. Prat, High-throughput, quantitative assessment of the effects of low-dose silica nanoparticles on lung cells: grasping complex toxicity with a great depth of field, BMC Genomics, 16 (2015) 315. https://doi.org/10.1186/s12864-015-1521-5
[37] N. Decan, D. Wu, A. Williams, S. Bernatchez, M. Johnston, M. Hill, S. Halappanavar, Characterization of in vitro genotoxic, cytotoxic and transcriptomic responses following exposures to amorphous silica of different sizes, Mutation Research/Genetic Toxicology and Environmental Mutagenesis, 796 (2016) 8-22. https://doi.org/10.1016/j.mrgentox.2015.11.011
[38] N.Q. Vuong, P. Goegan, F. De Rose, D. Breznan, E.M. Thomson, J.S. O'Brien, S. Karthikeyan, A. Williams, R. Vincent, P. Kumarathasan, Responses of A549 human lung epithelial cells to cristobalite and α-quartz exposures assessed by toxicoproteomics and gene expression analysis, Journal of Applied Toxicology, 37 (2017) 721-731. https://doi.org/10.1002/jat.3420
[39] M. Fang, Y. Li, K. Huang, S. Qi, J. Zhang, W. Zgodzinski, M. Majewski, G. Wallner, S. Gozdz, P. Macek, A. Kowalik, M. Pasiarski, E. Grywalska, L. Vatan, N. Nagarsheth, W. Li, L. Zhao, I. Kryczek, G. Wang, Z. Wang, W. Zou, L. Wang, IL33 Promotes Colon Cancer Cell Stemness via JNK Activation and Macrophage Recruitment, Cancer Research, 77 (2017) 2735-2745. https://doi.org/10.1158/0008-5472.Can-16-1602
[40] S. Karthikeyan, A. Russo, M. Dean, D.D. Lantvit, M. Endsley, J.E. Burdette, Prolactin signaling drives tumorigenesis in human high grade serous ovarian cancer cells and in a

586 spontaneous fallopian tube derived model, Cancer Letters, 433 (2018) 221-231.
587 https://doi.org/10.1016/j.canlet.2018.07.003
588 [41] D. Senfter, E.P. Erkan, E. Özer, G. Jungwirth, S. Madlener, M. Kool, T. Ströbel, N.
589 Saydam, O. Saydam, Overexpression of minichromosome maintenance protein 10 in
590 medulloblastoma and its clinical implications, Pediatric Blood & Cancer, 64 (2017) e26670.
591 https://doi.org/10.1002/pbc.26670
592 [42] W.M. Li, C.N. Huang, H.L. Ke, C.C. Li, Y.C. Wei, H.C. Yeh, L.L. Chang, C.H. Huang,
593 P.I. Liang, B.W. Yeh, T.C. Chan, C.F. Li, W.J. Wu, MCM10 overexpression implicates
594 adverse prognosis in urothelial carcinoma, Oncotarget, 7 (2016) 77777-77792.
595 https://doi.org/10.18632/oncotarget.12795
596 [43] F. Cui, J. Hu, S. Ning, J. Tan, H. Tang, Overexpression of MCM10 promotes cell
597 proliferation and predicts poor prognosis in prostate cancer, The Prostate, 78 (2018) 1299-
598 1310. https://doi.org/10.1002/pros.23703
599 [44] R. Mahadevappa, H. Neves, S.M. Yuen, M. Jameel, Y. Bai, H.-F. Yuen, S.-D. Zhang, Y.
600 Zhu, Y. Lin, H.F. Kwok, DNA Replication Licensing Protein MCM10 Promotes Tumor
601 Progression and Is a Novel Prognostic Biomarker and Potential Therapeutic Target in Breast
602 Cancer, Cancers, 10 (2018) 282. https://doi.org/10.3390/cancers10090282
603 [45] A.S. Lieu, T.S. Cheng, C.H. Chou, C.H. Wu, C.Y. Hsu, C.Y. Huang, L.K. Chang, J.K.
604 Loh, C.S. Chang, C.M. Hsu, S.L. Howng, Y.R. Hong, Functional characterization of AIBp, a
605 novel Aurora-A binding protein in centrosome structure and spindle formation, Int J Oncol,
606 37 (2010) 429-436. https://doi.org/10.3892/ijo_00000691
607 [46] S. Ueda, I. Kuwabara, F.T. Liu, Suppression of tumor growth by galectin-7 gene transfer,
608 Cancer Research, 64 (2004) 5672–5676. https://doi.org/10.1158/0008-5472.CAN-04-0985
609 [47] S.J. Kim, J.A. Hwang, J.Y. Ro, Y.S. Lee, K.H. Chun, Galectin-7 is epigenetically-
610 regulated tumor suppressor in gastric cancer, Oncotarget, 4 (2013) 1461–1471.
611 https://doi.org/10.18632/oncotarget.1219
612 [48] K. Biron-Pain, A.-A. Grosset, F. Poirier, L. Gaboury, Y. St-Pierre, Expression and
613 Functions of Galectin-7 in Human and Murine Melanomas, PLoS One, 8 (2013) e63307.
614 https://doi.org/10.1371/journal.pone.0063307
615 [49] C.J. Kim, N. Yoshioka, Y. Tambe, R. Kushima, Y. Okada, H. Inoue, Periostin is down-
616 regulated in high grade human bladder cancers and suppresses in vitro cell invasiveness and
617 in vivo metastasis of cancer cells, International Journal of Cancer, 117 (2005) 51-58.
618 https://doi.org/10.1002/ijc.21120
619 [50] P. Li, J. Qian, G. Yu, Y. Chen, K. Liu, J. Li, J. Wang, Down-regulated SPARCL1 is
620 associated with clinical significance in human gastric cancer, Journal of Surgical Oncology,
621 105 (2012) 31-37. https://doi.org/10.1002/jso.22025
622 [51] F. Cao, K. Wang, R. Zhu, Y.W. Hu, W.Z. Fang, H.Z. Ding, Clinicopathological
623 significance of reduced SPARCL1 expression in human breast cancer, Asian Pacific Journal
624 of Cancer Prevention, 14 (2013) 195-200. https://doi.org/10.7314/apjcp.2013.14.1.195
625 [52] P.J. Hurley, L. Marchionni, B.W. Simons, A.E. Ross, S.B. Peskoe, R.M. Miller, N. Erho,
626 I.A. Vergara, M. Ghadessi, Z. Huang, B. Gurel, B.H. Park, E. Davicioni, R.B. Jenkins, E.A.
627 Platz, D.M. Berman, E.M. Schaeffer, Secreted protein, acidic and rich in cysteine-like 1
628 (SPARCL1) is down regulated in aggressive prostate cancers and is prognostic for poor
629 clinical outcome, Proceedings of the National Academy of Sciences, 109 (2012) 14977-
630 14982. https://doi.org/10.1073/pnas.1203525109
631 [53] P. Lévy, D. Vidaud, K. Leroy, I. Laurendeau, J. Wechsler, G. Bolasco, B. Parfait, P.
632 Wolkenstein, M. Vidaud, I. Bièche, Molecular profiling of malignant peripheral nerve sheath
633 tumors associated with neurofibromatosis type 1, based on large-scale real-time RT-PCR,
634 Molecular Cancer, 3 (2004) 20. https://doi.org/10.1186/1476-4598-3-20

635 [54] B. Kigel, A. Varshavsky, O. Kessler, G. Neufeld, Successful Inhibition of Tumor
636 Development by Specific Class-3 Semaphorins Is Associated with Expression of Appropriate
637 Semaphorin Receptors by Tumor Cells, PLoS One, 3 (2008) e3287.
638 https://doi.org/10.1371/journal.pone.0003287
639 [55] X. Zhou, L. Ma, J. Li, J. Gu, Q. Shi, R. Yu, Effects of SEMA3G on migration and
640 invasion of glioma cells, Oncology Reports, 28 (2012) 269-275.
641 https://doi.org/10.3892/or.2012.1796
642 [56] M. Dutertre, L. Gratadou, E. Dardenne, S. Germann, S. Samaan, R. Lidereau, K.
643 Driouch, P. de la Grange, D. Auboeuf, Estrogen Regulation and Physiopathologic
644 Significance of Alternative Promoters in Breast Cancer, Cancer Research, 70 (2010) 3760-
645 3770. https://doi.org/10.1158/0008-5472.Can-09-3988
646 [57] I. Kuwabara, Y. Kuwabara, R.Y. Yang, M. Schuler, D.R. Green, B.L. Zuraw, D.K. Hsu,
647 F.T. Liu, Galectin-7 (PIG1) exhibits pro-apoptotic function through JNK activation and
648 mitochondrial cytochrome cRelease, Journal of Biological Chemistry, 277 (2002) 3487-3497.
649 https://doi.org/10.1074/jbc.M109360200
650 [58] P.J. Neame*, C.J. Kay, D.J. McQuillan, M.P. Beales, J.R. Hassell, Independent
651 modulation of collagen fibrillogenesis by decorin and lumican, Cellular and Molecular Life
652 Sciences CMLS, 57 (2000) 859-863. https://doi.org/10.1007/s000180050048
653 [59] S. Chattopadhyay, A.-K. Bielinsky, Human Mcm10 Regulates the Catalytic Subunit of
654 DNA Polymerase-α and Prevents DNA Damage during Replication, Molecular Biology of the
655 Cell, 18 (2007) 4085-4095. https://doi.org/10.1091/mbc.e06-12-1148
656 [60] L. Gillan, D. Matei, D.A. Fishman, C.S. Gerbin, B.Y. Karlan, D.D. Chang, Periostin
657 Secreted by Epithelial Ovarian Carcinoma Is a Ligand for αVβ3 and αVβ5 Integrins and
658 Promotes Cell Motility, Cancer Research, 62 (2002) 5358-5364.
659 [61] X. Liu, S. Li, F. Yi, Trop2 gene: a novel target for cervical cancer treatment, Journal of
660 Cancer Research and Clinical Oncology, 140 (2014) 1331–1341.
661 https://doi.org/10.1007/s00432-014-1696-1
662 [62] M.M. Sullivan, T.H. Barker, S.E. Funk, A. Karchin, N.S. Seo, M. Höök, J. Sanders, B.
663 Starcher, T.N. Wight, P. Puolakkainen, E.H. Sage, Matricellular Hevin Regulates Decorin
664 Production and Collagen Assembly, Journal of Biological Chemistry, 281 (2006) 27621-
665 27632. https://doi.org/10.1074/jbc.M510507200
666 [63] L. Huang, Y. Xu, G. Cai, Z. Guan, S. Cai, Downregulation of S100A4 expression by
667 RNA interference suppresses cell growth and invasion in human colorectal cancer cells,
668 Oncology Reports, 27 (2012) 917-922. https://doi.org/10.3892/or.2011.1598
669 [64] K. Rasmussen, J.M. Mech, J. Mast, Synthetic Amorphous Silicon Dioxide (NM-200,
670 NM-201, NM-202, NM-203, NM-204): Characterisation and Physico-Chemical Properties.
671 JRC Repository: NM-series of Representative Manufactured Nanomaterials, Publications
672 Office of the European Union, Luxembourg, (2013) 200.
673 [65] Z. Elias, O. Poirot, I. Fenoglio, M. Ghiazza, M.C. Daniere, F. Terzetti, C. Darne, C.
674 Coulais, I. Matekovits, B. Fubini, Surface reactivity, cytotoxic, and morphological
675 transforming effects of diatomaceous Earth products in Syrian hamster embryo cells, Toxicol
676 Sci, 91 (2006) 510-520. https://doi.org/kfj177 [pii]
677 10.1093/toxsci/kfj177
678

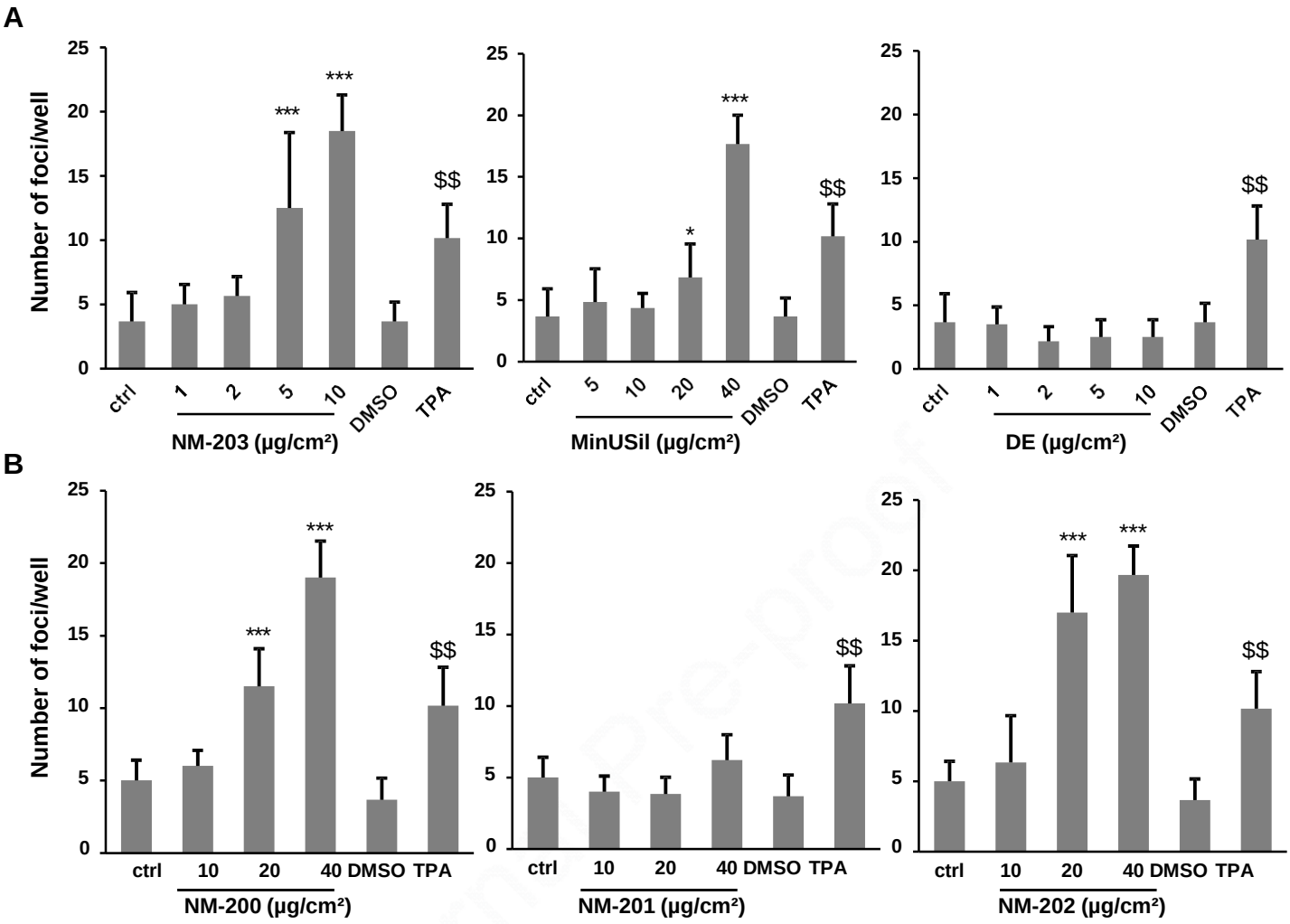

Figure 1: Bhas 42 cell transformation assay.

(**A**). Bhas 42 cells were treated once with increasing concentrations of NM-203, Min-U-Sil 5® or DE cultivated over 21 days. Foci, resulting from cell transformation, were counted as described in the *materials and methods* section. **B**). Similar experiments were performed with NM-200, NM-201 and NM-202. The values obtained after cell exposure to TPA (0.05 µg/ml) or DMSO (used as the vehicle for TPA), were added to each histogram. Results are expressed as the mean ± SD (n = 6). ***: $p < 0.005$, comparison of results obtained from cells exposed to nanoparticle *versus* cells treated with H_2O (ctrl). $$: $p < 0,01$, comparison of results obtained from cells exposed to TPA *versus* cells treated with DMSO after mixed linear regression modelling followed by a Bonferroni correction.

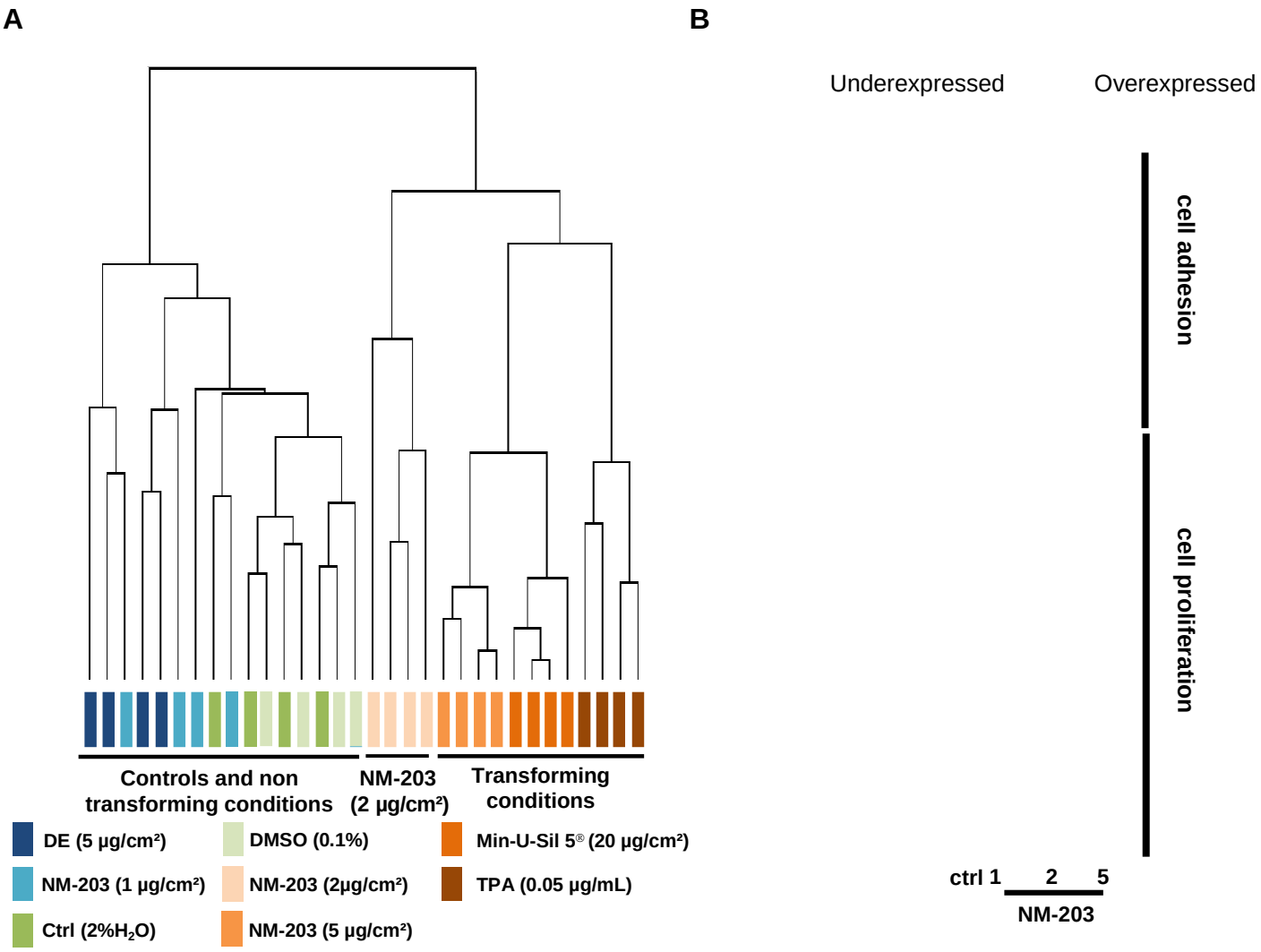

Figure 2: Hierarchical clustering of Bhas42 cells after treatments.

Cells were exposed to NM-203 (1, 2 or 5 µg/cm²), Min-U-Sil 5® (20 µg/cm²), DE (5 µg/cm²) and TPA (0.05 µg/mL). (**A**) A non supervised hierarchical cluster was obtained after filtering microarray data, using Gene Cluster 3.0 software on 19569 probes. Gene clustering was visualized with Treeview. An uncentred correlation was used as a measure of similarity and complete linkage was used for the clustering method. (**B**) Dose effect of NM-203 (1-5 µg/cm²). Supervised hierarchical clustering was performed with Gene Cluster 3.0 software and visualized by Treeview on the 285 probes obtained after filtration and application of the ANOVA statistical test (p-value < 0.005 and FC > 4), by comparing NM-203 (1 µg / cm²), NM-203 (2 µg / cm²) and NM-203 (5 µg / cm²) and control H_2O, followed by a Tukey post-hoc test. An uncentred correlation was used as a measure of similarity and complete linkage was used for the clustering method. Green indicates lower expression; red indicates higher expression. Biological functions related to the main clusters were evaluated using the FuncAssociate 2.0 program. (Abbreviations: Ctrl, control (H_2O); TPA, 12-*O*-tetradecanoylphorbol-13-acetate: DE. diatomaceous earth; DMSO, dimethyl sulfoxide.

A

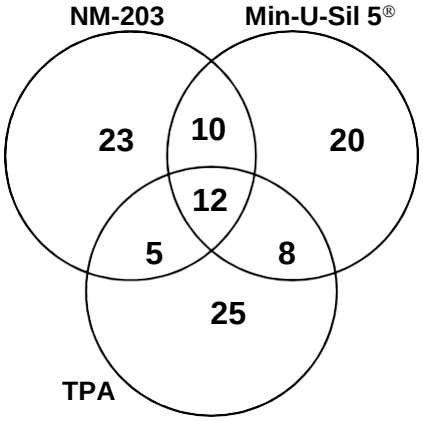

B

12 common signatures
FISCHER_G1_S_CELL_CYCLE_UP
FERREIRA_EWINGS_SARCOMA_UNSTABLE_VS_STABLE_UP
LINDGREN_BLADDER_CANCER_CLUSTER_3_UP
VECCHI_GASTRIC_CANCER_EARLY_UP
DUTERTRE_ESTRADIOL_RESPONSE_24HR_UP
CHEMNITZ_RESPONSE_TO_PROSTAGLANDIN_E2_UP
BASAKI_YBX1_TARGETS_UP
FUJII_YBX1_TARGETS_DN
FURUKAWA_DUSP6_TARGETS_PCI35_DN
ODONNELL_TFRC_TARGETS_DN
BHATI_G2M_ARREST_BY_2METHOXYESTRADIOL_UP
GOBERT_OLIGODENDROCYTE_DIFFERENTIATION_UP

C

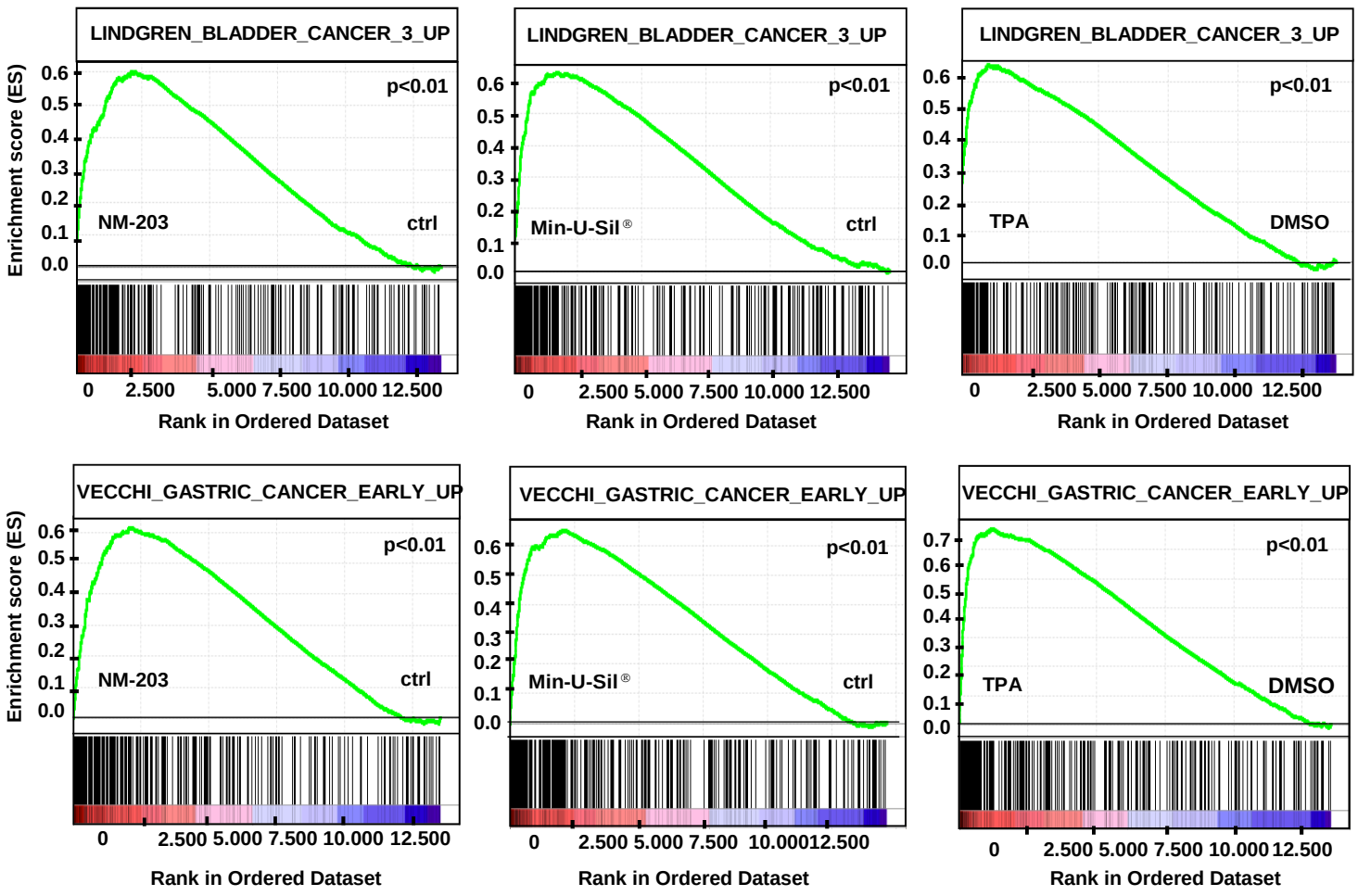

Figure 3: Gene set enrichment analysis.

(A) GSEA analysis using the filtered gene expression profiles of Bhas 42 cells 48h after treatment with NM-203 (5 µg/cm^2), Min-U-Sil 5® (20 µg/cm^2) and TPA (0.05 µg/ml) over 48 hours. Venn diagram of the top 50 signatures. (**B**) List of the 12 common signatures. **(C)** GSEA revealed an enrichment in gene signatures related to cell cycles and cancer that was common to the three conditions, for example the "Lindgren_bladder_cancer_3_up" signature (upper panels), and the "Vecchi_gastric_cancer_early_up" signature (lower panels).

A

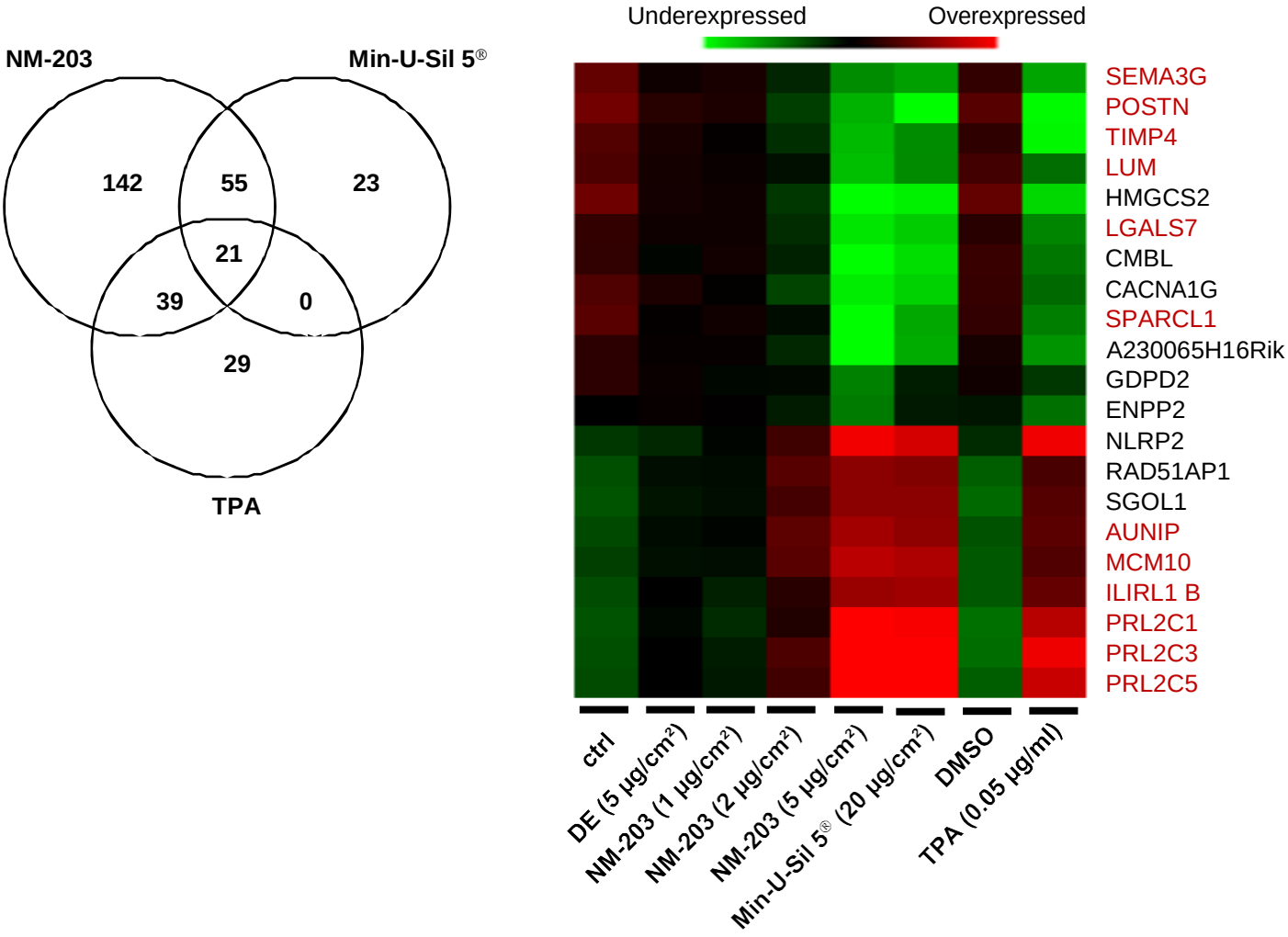

Figure 4: Molecular signature comparison and selection of common genes.

(A) : Venn diagram comparing the molecular signatures of NM-203 (5 µg/cm²), Min-U-Sil 5® (20 µg/cm²) and TPA (0.05 µg/mL) ($p < 0.005$ and FC > 4). (**B**): Heatmap of 21 common genes regulated by the three transforming compounds obtained with Gene Cluster 3.0 software and visualized with Treeview. An average of the expression of each gene was obtained for each condition. Green indicates the lower gene expression; red the higher gene expression. The writing in red corresponds to the selected genes of interest. (Abbreviations: ctrl, control H_2O, TPA, 12-*O*-tetradecanoylphorbol-13-acetate; DMSO, dimethyl sulfoxide; DE, diatomaceous earth).

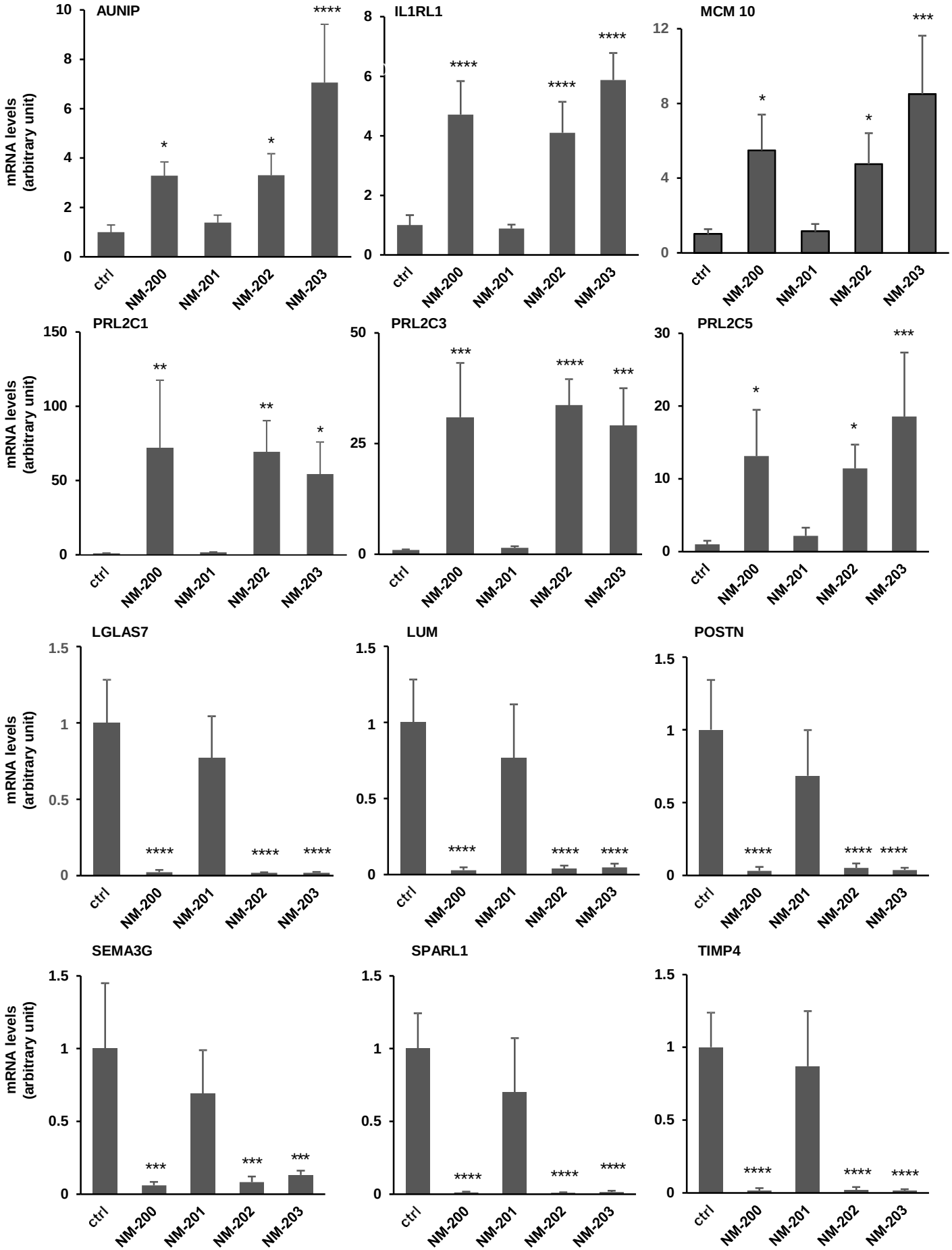

Figure 5: Expression changes induced by silica nanoparticles NM-200, NM-201 and NM-202.
Relative expression of the 12 selected genes (*AUNIP, IL1RL1 (Isoform B), MCM10, PRL2C1, PRL2C3, PRL2C5, LGLAS7, LUM, POSTN, SEMA3G, SPARL1 and TIMP4*) after 48h-treatment of Bhas 42 cells with NM-200 (20 µg/cm²), NM-201 (20 µg/cm²), NM-202 (20 µg/cm²) and NM203 (5 µg/cm²). The results are presented with respect to those of control cells taken as 1.00. The results are expressed as the mean of four independent experiments. * indicates $p < 0.05$, ** indicates $p < 0.01$, *** indicates $p < 0.005$, **** indicates $p < 0.001$ *versus* control cells after a one-way ANOVA test followed by a Dunnett's multiple comparisons test. (Abbreviations: Ctrl, control (H_2O)).

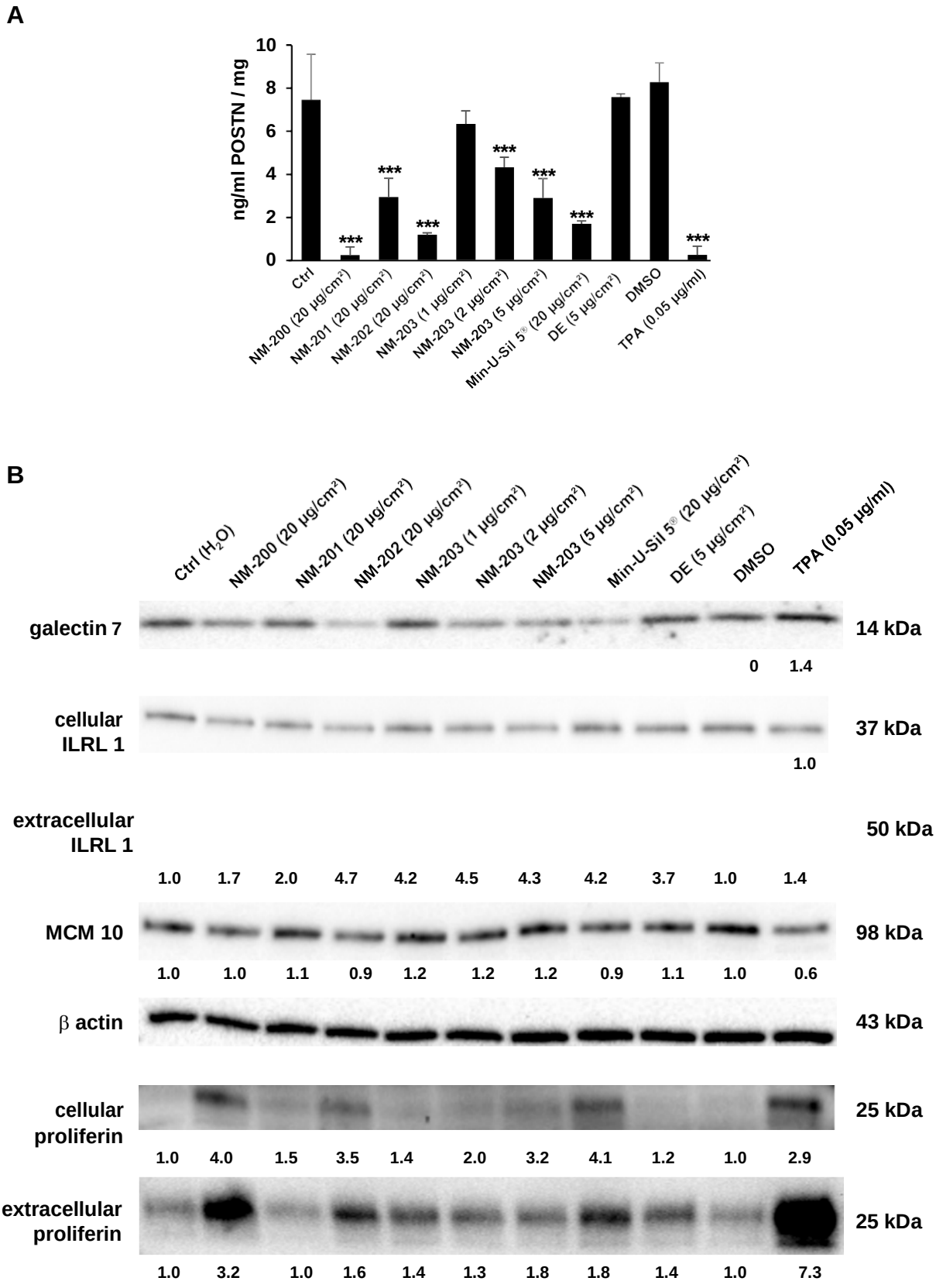

Figure 6: Protein analysis.

A) Periostin secretion (POSTN) was determined by ELISA in supernatants from cell layers exposed to each nanoparticle over 48 h. *** , $p < 0.005$ (n =3) with respect to the control (ctrl = H_2O) or DMSO (used as the vehicle for the particles or TPA, respectively), following a mixed linear regression model followed by a Bonferroni multiple comparison test. Results are expressed as ng of POSTN/ ml of supernatant harvested normalized to mg of protein in the respective cell homogenate. (**B**) Protein levels were analysed by Western blotting using cell homogenates. Proliferin and ILR1 were also detected in the cell culture supernatant from treated cells. Results are representative of one out of three independent experiments. β-actin was used as a loading control in each blot, with the exception of extracellular proliferin or IL1R1 detection in cell supernatant.